doi:10.2533/chimia.2012.201 Chimia 66 (2012) 201–204

Development of [^{18}F]-PSS223 as a PET Tracer for Imaging of Metabotropic Glutamate Receptor Subtype 5 (mGluR5)

Selena Milicevic Sephton§, Patrick Dennler, Dominique S. Leutwiler, Linjing Mu, Roger Schibli, Stefanie D. Krämer, and Simon M. Ametamey*

§SCS-Metrohm Foundation Award for best oral presentation

Abstract: Involvement of metabotropic glutamate receptor subtype 5 (mGluR5) in physiological and pathophysiological processes in the brain has been demonstrated, and hence mGluR5 has emerged as an important drug target. [^{11}C]-ABP688 is clinically the most successful mGluR5 positron emission tomography (PET) tracer to date and it allows visualization and quantification of mGluR5. Due to the short half-life of carbon-11, clinical use of [^{11}C]-ABP688 is limited to facilities with an on-site cyclotron and a fluorine-18 (half-life 110 min) analogue would be more practical. Based on the [^{11}C]-ABP688 structural motif, a novel derivative [^{18}F]-PSS223 was prepared and evaluated as a PET tracer for imaging of mGluR5 *in vitro* and *in vivo*. Our results show favourable *in vitro* binding properties; however rapid defluorination of [^{18}F]-PSS223 does not allow visualization of mGluR5 in the rat brain.

Keywords: [^{11}C]-ABP688 · [^{18}F]-FDEGPECO · [^{18}F]-PSS223 · mGluR5 · PET imaging

1. Introduction

The function of glutamate, a major neurotransmitter in the mammalian brain, is mediated through two types of receptors: ionotropic (*e.g.* NMDA, AMPA or kainate) and metabotropic (*e.g.* mGluR receptor family). Metabotropic glutamate receptors (mGluR) were identified in 1991 and they are divided in three groups based on sequence homology, receptor pharmacology and signal transduction: group I (mGluR1 and mGluR5), group II (mGluR2 and mGluR3), and group III (mGluR4 and mGluR6-8).[1–8] While ionotropic glutamate receptors are mainly involved with fast excitatory neurotransmission, mGluRs are responsible for subtle changes in neurotransmission. mGluR5 is a seven transmembrane domain G-protein coupled postsynaptically situated receptor. Studies have implicated mGluR5 with processes of learning and memory, but also involvement of mGluR5 in several disorders of the central nervous system (CNS) such as Alzheimer's and Parkinson's diseases, schizophrenia, depression and anxiety.[9–11] Although the precise mechanisms governing the involvement of mGluR5 in pathophysiological processes in the brain are not fully understood, mGluR5 is considered an important drug target and imaging of mGluR5 *in vivo* arose as a challenge to PET community.

Positron emission tomography (PET) is a powerful non-invasive imaging technique which is employed in the quantification of biochemical and pharmacodynamic processes in healthy and diseased states and is particularly important for the drug development as it facilitates deeper understanding of drug-target interactions *in vivo* and monitoring of effects of drug candidates on the progression of a disease.[12] For these reasons, development of a PET radiotracer for mGluR5 is advantageous and several mGluR5 PET tracers have been developed to date. Clinically the most successful radiotracer for imaging of mGluR5 is (*E*)-3-((6-methylpyridin-2-yl) ethynyl)cyclohex-2-enone-*O*-^{11}C-methyl oxime ([^{11}C]-ABP688),[13,14] developed by the Ametamey group and exhibited excellent *in vitro* and *in vivo* properties; however the application of [^{11}C]-ABP688 is limited to facilities with an on-site cyclotron due to the extremely short half-life of carbon-11 (20 min). In order to overcome this limitation scientific efforts were made towards the development of an analogous fluorine-18 radiotracer which would have a physical half-life of 110 min. [^{18}F]-SP203[15–17] and [^{18}F]-FPEB[18,19] are two radiotracers for imaging of mGluR5 developed by the Pike and Hamill groups, respectively; however they both have shortcomings, first due to defluorination in human subjects albeit in modest amount and the latter due to tedious radiosynthesis (Fig. 1). Efforts from the Ametamey group were aimed at developing a fluorine-18 analogue of [^{11}C]-ABP688 by the least number of structural changes which led to (*E*)-3-(pyridin-2-ylethynyl)cyclohex-2-enone *O*-(2-(2-^{18}F-fluoroethoxy)ethyl) oxime ([^{18}F]-FDEGPECO, Fig. 1).[20,21] The main advantages of [^{18}F]-FDEGPECO in comparison to other fluorine-18 radiotracers are based on the ease with which [^{18}F]-FDEGPECO is produced in a single high-yielding radiochemical step and good stability *in vivo* (*i.e.* no defluorination was observed in the dynamic PET scan); however although quantification of mGluR5 was possible, quality of the images was reduced by significant background.

One of the important criteria in designing new brain tracers is their lipophilicity, which among other parameters determines the successful passage across the blood brain barrier (BBB).[22] For mGluR5

*Correspondence: Prof. Dr. S. M. Ametamey
Center for Radiopharmaceutical Sciences of ETH, PSI and USZ
Department of Chemistry and Applied Biosciences
ETH-Hönggerberg
Wolfgang-Pauli Strasse 10
CH-8093 Zürich
Tel.: +41 1 633 7463
Fax: +41 1 633 1367
E-mail: simon.ametamey@pharma.ethz.ch

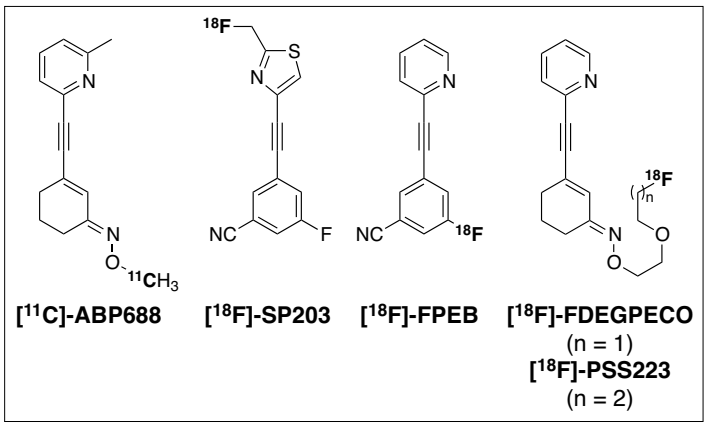

Fig. 1. Selected carbon-11 and fluorine-18 PET tracers for imaging of mGluR5.

our group established an optimal range of logD values (1.7–2.5)[20] and [^{18}F]-FDEGPECO exhibited a logD slightly lower than desired. We hypothesized that by extending the lipophilic side chain in [^{18}F]-FDEGPECO by one methylene unit, the increased lipophilicity of this novel derivative (*E*)-3-(pyridin-2-ylethynyl)cyclohex-2-enone *O*-(2-(3-^{18}F-fluoropropoxy) ethyl) oxime ([^{18}F]-PSS223, Fig. 1) could in turn lead to a better signal-to-noise ratio in the PET image.

2. Synthesis of PSS223

The syntheses of both PSS223 and [^{18}F]-PSS223 were envisioned *via* nucleophilic substitutions of common precursor **1** with the corresponding nucleophilic fluoride sources (Scheme 1). The suitably functionalized intermediate **1** would be accessed *via* a coupling of oxime **3** and bromoether **2**.

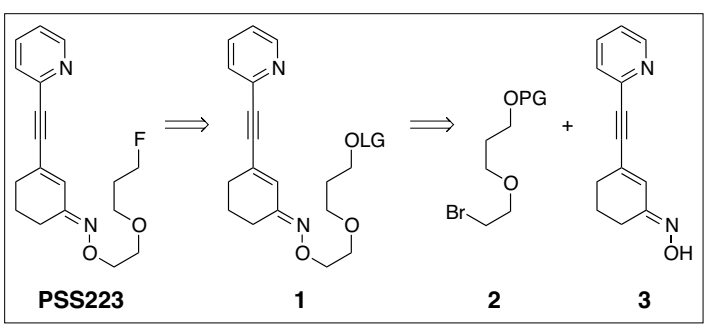

Scheme 1. Retrosynthetic analysis for the synthesis of PSS223; PG – protecting group; LG – leaving group.

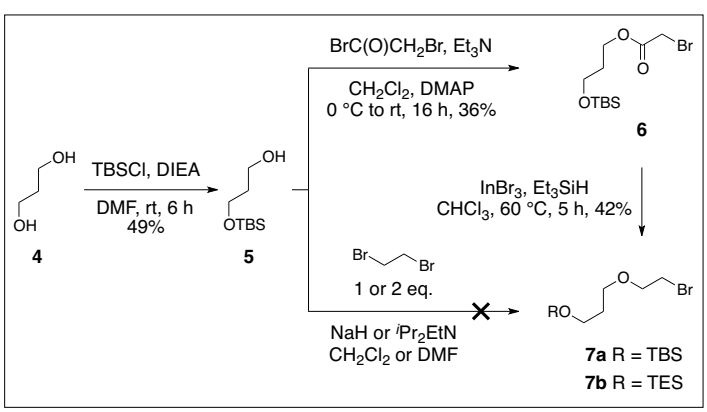

Scheme 2. Synthesis of bromoether **7**.

To form bromoether **2** the commercially available 1,3-propanediol (**4**) was monoprotected to yield TBS silyl ether **5**. Several attempts to obtain the coupling partner **7** directly using dibromoethane failed and a two-step approach *via* bromoester **6** afforded bromoether **7** after reduction of the ester functionality with triethylsilane/indium(III)-bromide[23] (Scheme 2) in 7% yield over three steps.[24] Interestingly, **7** was isolated as a mixture of TBS- and TES-silylethers **7a** and **7b**, respectively, presumably from the exchange of silyl-ether groups. Although it was possible to separate **7a** and **7b** *via* column chromatography, for the next step the mixture of silylethers was successfully employed.

Oxime **3** was synthesized from commercially available 3-ethoxy-cyclohex-2-enone (**8**) which was converted to acetylene **9** in 93% yield and further reacted with hydroxylamine to give a 3:1 ratio of *E*- and *Z*-oximes (*E*)-**10** and (*Z*)-**10**, respectively.[20,25] The mixture was successfully separated by column chromatography and the major isomer (*E*) was coupled to bromopyridine under Sonogashira reaction conditions (Scheme 3).

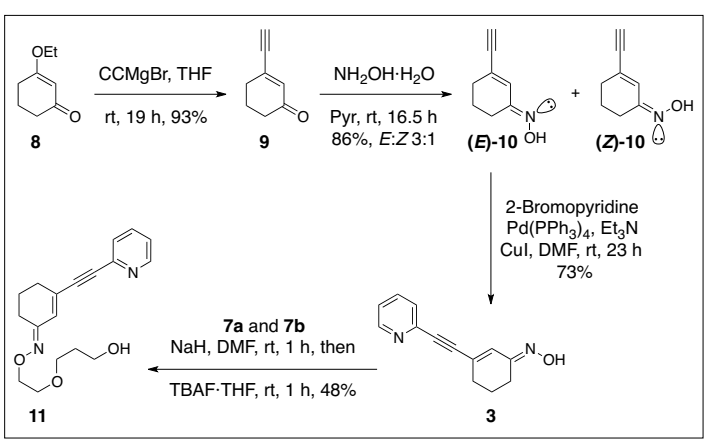

Scheme 3. Synthesis of alcohol **11**.

The mixture of bromoethers **7a** and **7b** was then reacted with oxime **3** and the crude mixture of silylethers was immediately deprotected using a TBAF·THF complex to furnish alcohol **11** with an overall yield of 28% (five steps). With alcohol **11** in hand, we next sought an optimal leaving group. Initially, **11** was converted to tosylate **12** in 65% yield, however attempts to substitute the tosyl group in **12** with fluoride resulted only in decomposition of **12** (Scheme 4). Alcohol **11** was then converted to mesylate **13** with a higher yield (85%), reduced reaction time and successfully substituted to form PSS223 with potassium fluoride in 70% yield (Scheme 4).

3. Radiolabelling of 10

Mesylate **13** was also used to obtain [^{18}F]-PSS223 in one step using an aqueous solution of $^{18}F^-$ complexed with Kryptofix-222® and K_2CO_3 as a nucleophilic source of fluoride at 90 °C over 10 min (Scheme 5).[24] [^{18}F]-PSS223 was purified *via* semi-preparative HPLC and the collected product was then trapped on a C18 cartridge to remove acetonitrile used for HPLC purification. The labelled product was eluted with ethanol and the ethanolic solution of [^{18}F]-PSS223 was diluted with PEG:H_2O 1:1 to give 5–6 GBq (20%

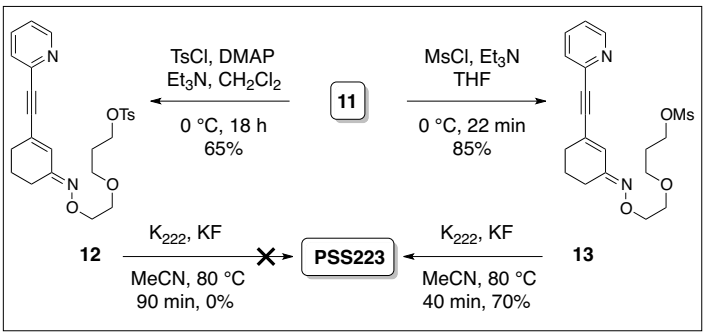

Scheme 4. Synthesis of cold PSS223.

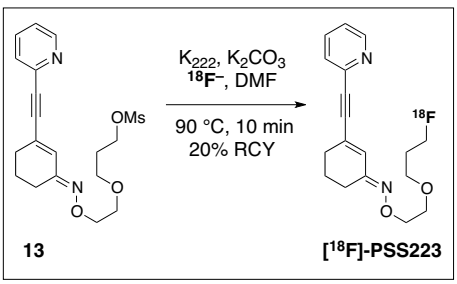

Scheme 5. Radiolabelling of mesylate **13** to yield [^{18}F]-PSS223.

decay corrected radiochemical yield) of >97% pure formulated product with specific activity ranging between 100–320 GBq/µmol.

4. *in vitro* Evaluation of [^{18}F]-PSS223

The *in vitro* evaluation of [^{18}F]-PSS223 involved determining the binding affinity and *in vitro* autoradiography with rat brain slices. For CNS tracers the ideal binding affinity is below 2 nM with a tolerance of 5 nM, to comply with the criteria of B_{max}/K_d >>1.[22] The K_d for [^{18}F]-PSS223 was estimated from the saturation binding assay as 3.34±2.05 nM,[24] suggesting excellent binding of [^{18}F]-PSS223 to mGluR5.

In vitro autoradiography was performed on horizontal rat brain slices with a 1 nM solution of [^{18}F]-PSS223 and resulted in heterogeneous distribution of radioactivity with highest signals in the regions where mGluR5 is highly expressed (*i.e.* striatum, hippocampus and cortex). MGluR5 shows low expression in the cerebellum[1,3,5] and the radioactivity in this region was at the background level (Fig. 2a). To establish specificity of [^{18}F]-PSS223 for mGluR5, incubation of brain slices was conducted with a solution containing 1 nM of radiotracer and 100 nM of cold ABP688, which specifically binds to mGluR5. A complete blocking of the radioactivity signals in mGluR5 brain regions was observed (Fig. 2b). Stability of [^{18}F]-PSS223 towards rat liver microsomal enzymes was investigated and it was found that 90% of the parent radiotracer was metabolized over one hour suggesting rapid metabolism *in vivo*.

5. *in vivo* Evaluation of [^{18}F]-PSS223

We next explored [^{18}F]-PSS223 in an *in vivo* dynamic PET scan. Time–activity curves obtained from the *in vivo* imaging are depicted in Fig. 3. Significant accumulation of radioactivity was observed in the jaws over the duration of the scan (90 min) suggesting rapid defluorination of [^{18}F]-PSS223. Likely mechanisms for the rapid metabolism of [^{18}F]-PSS223 include oxidation by cytochrome P450.[24]

6. Conclusion

In conclusion, we have successfully synthesized PSS223, a novel ^{18}F-fluorine containing derivative based on the ABP688 structural motif which showed excellent binding affinity for mGluR5. Employing the same key intermediate **13** as the precursor, [^{18}F]-PSS223 was prepared in a single radiochemical step with 20% decay corrected yield. *In vitro* evaluation of [^{18}F]-PSS223 revealed excellent binding potential of our novel tracer; however incubation of [^{18}F]-PSS223 with rat microsomal enzymes suggested fast metabolism and the *in vivo* analysis confirmed rapid defluorination as reflected by accumulation of radioactivity in the skull and jaws. Further efforts are ongoing to discover an ^{18}F-labelled alternative to [^{11}C]-ABP688 with favourable *in vitro* and improved *in vivo* profile suitable for clinical use.

Acknowledgements

S. M. S. would like to acknowledge the Swiss Chemical Society and Metrohm AG for the award. The authors would like to acknowledge Mrs. Claudia Keller and Mrs. Petra Wirth for technical assistance in the PET lab. Prof. P. A. Schubiger, Dr. Cindy Wanger-Baumann, Miss Cindy Fischer and Dr. Thomas Betzel are acknowledged for support and many fruitful discussions.

Received: January 9, 2012

[1] P. J. Conn, J. P. Pin, *Annu. Rev. Pharmacol.* **1997**, *37*, 205.
[2] L. P. Daggett, A. I. Sacaan, M. Akong, S. P. Rao, S. D. Hess, C. Liaw, A. Urrutia, C. Jachec, S. B. Ellis, J. Dreessen, T. Knopfel, G. B. Landwehrmeyer, C. M. Testa, A. B. Young, M. Varney, E. C. Johnson, G. Velicelebi, *Neuropharmacology* **1995**, *34*, 871.
[3] M. Masu, Y. Tanabe, K. Tsuchida, R. Shigemoto, S. Nakanishi, *Nature* **1991**, *349*, 760.
[4] T. Ohnuma, S. J. Augood, H. arai, P. J. McKenna, P. C. Emson, *Mol. Brain Res.* **1998**, *56*, 207.

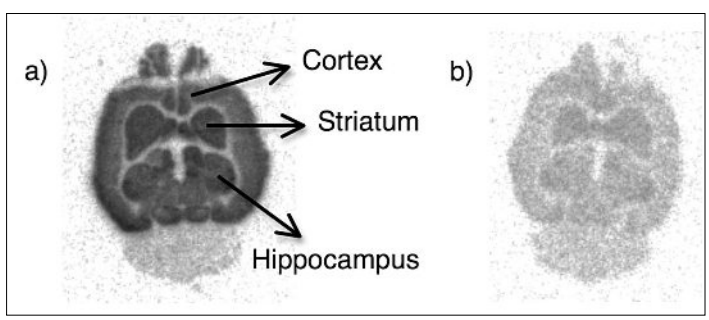

Fig. 2. *In vitro* autoradiography of [^{18}F]-PSS223 on horizontal rat brain slices: a) incubation of slices with 1 nM [^{18}F]-PSS223; b) incubation of slices with 1 nM [^{18}F]-PSS223 and 100 nM ABP688.

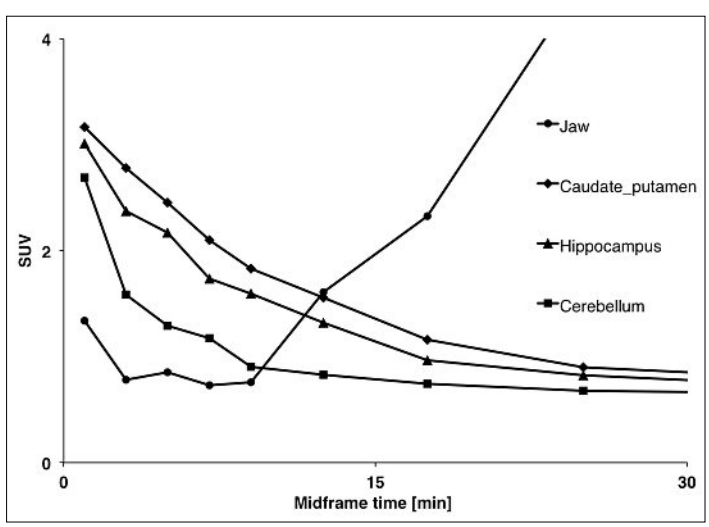

Fig. 3. Time-activity curves for [^{18}F]-PSS223 in different rat brain regions and the jaws.

[5] J. P. Pin, R. Duvoisin, *Neuropharmacology* **1995**, *34*, 1.
[6] R. Shigemoto, N. Mizuno, *Handbook of Chemical Neuroanatomy* **2000**, *18*, 63.
[7] R. Shigemoto, S. Nomura, H. Ohishi, H. Sugihara, S. Nakanishi, N. Mizuno, *Neurosci. Lett.* **1993**, *163*, 53.
[8] Y. Tanabe, M. Masu, T. Ishii, R. Shigemoto, S. Nakanishi, *Neuron* **1992**, *8*, 169.
[9] C. Chiamulera, M. P. Epping-Jordan, A. Zocchi, C. Marcon, C. C. Cottiny, S. Tacconi, M. Corsi, F. Orzi, F. O. Conquet, *Nat. Neurosci.* **2001**, *4*, 873.
[10] F. Dorri, D. R. Hampson, A. Baskys, J. M. Wojtowicz, *Exp. Neurol.* **1997**, *147*, 48.
[11] Y. M. Lu, Z. Jia, C. Janus, J. T. Henderson, R. Gerlai, J. M. Wojtowicz, J. C. Roder, *J. Neurosci.* **1997**, *17*, 5196.
[12] S. M. Ametamey, M. Honer, P. A. Schubiger, *Chem. Rev*. **2008**, *108*, 1501.
[13] S. M. Ametamey, L. J. Kessler, M. Honer, M. T. Wyss, A. Buck, S. Hintermann, Y. P. Auberson, F. Gasparini, P. A. Schubiger, *J. Nucl. Med.* **2006**, *47*, 698.
[14] S. M. Ametamey, V. Treyer, J. Streffer, M. T. Wyss, M. Schmidt, M. Blagoev, S. Hintermann, Y. Auberson, F. Gasparini, U. C. Fischer, A. Buck, *J. Nucl. Med.* **2007**, *48*, 247.
[15] A. K. Brown, Y. Kimura, S. S. Zoghbi, F. G. Simeon, J. S. Liow, W. C. Kreisl, A. Taku, M. Fujita, V. W. Pike, R. B. Innis, *J. Nucl. Med.* **2008**, *49*, 2042.
[16] H. U. Shetty, S. S. Zoghbi, F. G. Simeon, J. S. Liow, A. K. Brown, P. Kannan, R. B. Innis, V. W. Pike, *J. Pharmacol. Exp. Ther.* **2008**, *327*, 727.
[17] F. G. Simeon, A. K. Brown, S. S. Zoghbi, V. M. Patterson, R. B. Innis, V. W. Pike, *J. Med. Chem.* **2007**, *50*, 3256.
[18] T. G. Hamill, S. R. C. Krause, C. Bonnefous, S. Govek, T. G. Seiders, N. P. D. Cosford, J. Roppe, T. Kamenecka, S. Patel, R. E. Gibson, S. Sanabria, K. Riffel, W. Eng, C. King, X. Yang, M. D. Green, S. S. O'Malley, R. Hargreaves, H. D. Burns, *Synapse* **2005**, *56*, 205.
[19] J. Q. Wang, W. Tueckmantel, A. Zhu, D. Pellegrino, A. L. Brownell, *Synapse* **2007**, *61*, 951.
[20] C. A. Baumann, L. Mu, S. Johannsen, M. Honer, P. A. Schubiger, S. M. Ametamey, *J. Med. Chem.* **2010**, *53*, 4009.
[21] C. A. Wanger-Baumann, L. Mu, M. Honer, S. Belli, M. F. Alf, P. A. Schubiger, S. D. Kramer, S. M. Ametamey, *Neuroimage* **2011**, *56*, 984.
[22] W. C. Eckelman, R. E. Gibson, W. J. Rzeszotarski, F. Vieras, J. K. Mazaitis, B. Francis, W. C. Reba, 'The design of receptor binding radiotracers', CRC Press: New York, **1979**, Vol. 1, p. 251.
[23] N. Sakai, T. Moriya, K. Fujii, T. Konakahara, *Synthesis* **2008**, *21*, 3533.
[24] S. M. Sephton, P. Dennler, D. Leutwiler, L. Mu, C. A. Wanger-Baumann, R. Schibli, S. D. Krämer, S. M. Ametamey, *Am. J. Nucl. Med. Mol. Imaging* **2012**, *2*, 14.
[25] C. Lucatelli, M. Honer, J. F. Salazar, T. L. Ross, P. A. Schubiger, S. M. Ametamey, *Nucl. Med. Biol.* **2009**, *36*, 613.